# Novel biodegradable poly(gamma-glutamic acid)-amphotericin B complexes show promise as improved amphotericin B formulations

T. Dinh[1], Q. Zia[2], S. Zubair[2], P Stapleton[1], R. Singh[1], *M. Owais[2] and *S. Somavarapu[1]

[1] UCL School of Pharmacy, University College London, 29-39 Brunswick Square, London WC1N 1AX, UK.
[2] Interdisciplinary Biotechnology Unit, Aligarh Muslim University, Aligarh-202002, India

* Corresponding authors:
s.somavarapu@ucl.ac.uk;
owais_lakhnawi@yahoo.com

Abstract = 145 words

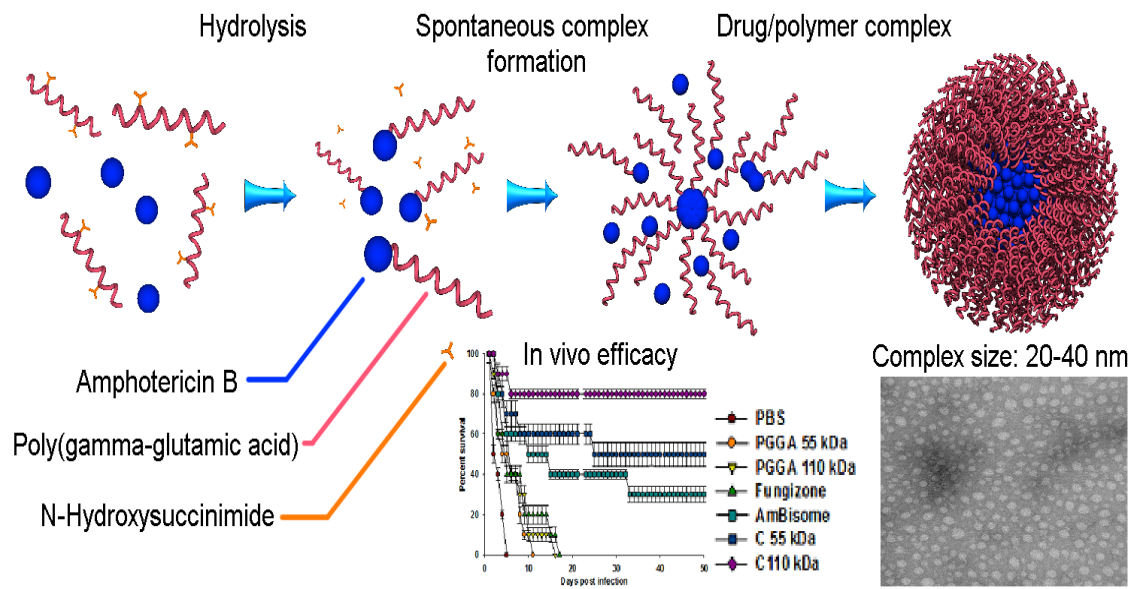Manuscript= 4818 (without references); 6413 (with references)

No. of references = 60

No. of figures = 7

No. of tables = 5

Supplement = 1568 words and 3 figures

## Graphical abstract



Hydrolysis

Spontaneous complex formation

Drug/polymer complex

Amphotericin B

Poly(gamma-glutamic acid)

N-Hydroxysuccinimide

In vivo efficacy

Complex size: 20-40 nm

- PBS
- PGGA 55 kDa
- PGGA 110 kDa
- Fungizone
- AmBisome
- C 55 kDa
- C 110 kDa

**ABSTRACT**

Commercially available amphotericin B (AmB) formulations are limited either by cytotoxicities, lower efficacies, shelf-life related issues or high production costs. AmB complexes based on poly(gamma-glutamic acid) (PGGA) have been prepared and evaluated for their efficacies against AmB-deoxycholate (Fungizone®) and liposomal AmB (AmBisome®). Physical characterizations showed that AmB/PGGA complexes are nanoscopic (20-40 nm) with a negative zetapotential (-51.0 mV), water-soluble, stable in solution (up to 4 weeks, at 4°C and 25°C), and have a theoretical drug loading (up to 76.9%). *In-vitro,* AmB/PGGA complexes exhibited an improved and comparable cytotoxicity profile as compared with Fungizone® and AmBisome® respectively, with respect to haemolytic activity and up-regulation of cytokine productions (TNF-α and IL-1ß). AmB/PGGA complexes were significantly more efficacious *in-vivo* than both Fungizone® and AmBisome® in experimental murine *candidiasis*. These results provide strong evidence that AmB/PGGA complexes have a better efficacy and safety profile than the currently approved AmB products.

*Abbreviations:* AmB = amphotericin B, DLS = Dynamic Light Scattering, TEM = Transmission Electron Microscopy, MW = Molecular Weight.

*Key words:* amphotericin B, poly(gamma-glutamic acid), AmB/PGGA complexes, Fungizone® and AmBisome®, toxicity.

**INTRODUCTION**

Despite its reported toxicity, the polyene antibiotic, amphotericin B (AmB), has found clinical applications in the treatment of systemic fungal infections in patients with cancer, AIDS, organ transplantation, and in parasitic disease [1]. Long term treatment with a conventional AmB therapy such as Fungizone® (from here on simply stated as Fungizone), is associated with high incidence of renal impairment and hepatotoxicity [2], [3]. The lipid-based formulations, Amphocil® (colloidal dispersion) AmBisome® (liposomes; from here on simply stated as AmBisome) and Abelcet® (lipid complex) are more tolerable, offer better protection against the renal damage than Fungizone and can be administered at a higher dosage in cases of severe systemic infections [4], [5]. AmBisome could be administered up to 3-5 mg/kg daily with lower incidences of nephrotoxicity as compared with Fungizone, which is only licensed for a daily dose of 1mg/kg [6], [7]. Although less nephrotoxic, the lipid-based AmB formulations are less efficacious than the conventional AmB formulations, meaning that higher doses are often required for desirable therapeutic effect which may subsequently lead to toxic manifestations [8].

AmB's inherent low aqueous solubility poses many hurdles in the development of a suitable oral or injectable formulation. Both passive and active targeting approaches have been employed for delivering AmB. Passive delivery of AmB can be achieved using various polymeric systems, which being particulate in nature, are avidly taken up by macrophages due to their scavenging property [9]. A plethora of reports have shown that the polymeric nanoparticles are readily phagocytosed by macrophages [10], [11], [12] leading to the passive accumulation of the drug in the liver and spleen (macrophage rich organs). Interestingly, macrophage uptake could be further enhanced by attaching target specific ligands onto the nanoparticles [13]. Few examples of these actively targeting AmB nanocarriers include the pH-sensitive conjugates of AmB-poly(ethylene glycol) which selectively releases AmB at target site [14], mannan or pullanan bearing liposomes loaded with AmB to target alveolar macrophages [15], and a mannose-coated lipid nanospheres of AmB for specific targeting to reticlulo-endothelial macrophages [16].

Several polymeric micelles based on diblock and triblock co-polymers [17], [18], [19] have the potential to solubilise AmB. However, micelles have the tendency to lose their integrity in serum mimicking conditions [20], [21], resulting in sudden

release, or burst, of drugs in an uncontrolled fashion [20], [22]. An additional issue is that the encapsulation in the polymeric micelles resulted in the decrease of *in vitro* antifungal activity of the drug [23], [17]. Other polymers such as polyvinyl-pyrrolidone possess the ability to complex AmB, but suffer from very low (0.249% w/w) AmB loading [24]. AmB–cyclodextrin complexes have shown improved water solubility [25] but demonstrate toxicity to human red blood cells [26].

Biocompatible and water-soluble polymers, both synthetic and naturally-occurring, have been extensively used to improve water solubility, optimise pharmacokinetics and improve drug efficacy and safety [27]. The naturally-occuring poly(gamma-glutamic acid) (PGGA) is known to be biodegradable, non-toxic, non-immunogenic [28], well-tolerated at high doses in preclinical studies [29], and importantly is chemically modifiable owing to the presence of the pendant carboxylic groups [30]. PGGA can be obtained in large amounts at low production costs through engineering and optimization of various microbial fermentation processes [31]. Herein, we describe the development and evaluation of alternative AmB formulations using PGGA as the delivery vehicle. Through physicochemical and biological characterizations, we have been able to confirm that the as-synthesized AmB/PGGA complexes have a better safety profile as compared to Fungizone *in vitro*, and greater antifungal efficacy than both Fungizone and Ambisome *in vivo*. The data suggests that by employing a non-covalently associated polymeric nanocarrier, it is possible to overcome problems associated with delivering a potent but highly cytotoxic and hydrophobic drug such as AmB.

**MATERIALS AND METHODS**

**AmB/PGGA complex synthesis**

<u>Degradation of high molecular weight PGGA</u>

In a typical alkaline hydrolysis reaction, PGGA of the free acid form (5 g, 34.45 mmol; 1500 kDa, Natto Biosciences) was dissolved in aqueous sodium bicarbonate (50 mL, 67.60 mM). The solution was heated to $90^{\circ}$C and NaOH (1.38 g, 34.45 mmol) was added. The solution was maintained at $90^{\circ}$C for 6 h, and then was left to cool to room temperature. The pH of the solution was adjusted to 7.0 with HCl, and subsequently treated with Amberlite resin (50 g, IR-120 H$^+$ type, 50 mesh Sigma-Aldrich). After 1 h, the Amberlite resin was separated from the mixture by filtration and washed with deionised water (50 mL). The filtrate was collected and kept at 2-8$^{\circ}$C for 2 days prior

to further filtration to facilitate the precipitation of the polymer. The precipitate was collected and excess water was removed from the precipitate by freeze-drying. Molecular weight (MW) determination was carried out by Gel permeation chromatography (GPC), while the purity of the sample was assessed by FT-IR.

<u>N-Hydroxysuccinimide (NHS) activation of PGGA</u>

In a typical reaction, degraded PGGA (5 g, 34.45 mmol) and NHS (1.98 g, 17.23 mmol, Sigma-Aldrich) were dissolved together in anhydrous DMSO (30 mL). NHS activation of PGGA was initiated by the drop wise addition of *N, N'*-diisopropylcarbodiimide (DIPC) (2.63 mL, 17.23 mmol, Sigma-Aldrich) at room temperature. After 20 h, the reaction was terminated and the reaction mixture was stored at 2-8°C for 24 h. Activated polymer was precipitated out in dehydrated acetone, and the precipitate was treated twice with ice-cold dehydrated acetone and once with dehydrated hexane. Dehydration of acetone and hexane was carried out by treatment with molecular sieve beads (3A type, 4-8 mm, Sigma-Aldrich). The precipitate was collected and dried under vacuum. The NHS content was determined by $^1$H-NMR spectroscopy using a Bruker Advance spectrometer

<u>Preparation of AmB/PGGA complexes</u>

In a typical complex preparation, NHS-activated PGGA (10 mg, 68.9 mmol; solubilised in DMSO (200 μL)) was added drop-wise to the AmB solution (7.0 mg, 7.47 mmol, Sigma-Aldrich; solubilised in 200 μL of DMSO) in a round bottom flask with stirring over 15 min. Sodium hydroxide (109 μL, 109 mmol) was added drop-wise to the reaction mixture, followed by water (1 mL), and the mixture was left to stir for 1 h at room temperature. After further dilution with water (3.5 mL), the resulting solution was purified by dialysis (Visking, MW cut-off 12,000 -14,000 kDa) against deionised water over 24 h. Finally, the dialysate was passed through a 0.2 μm filter (Millipore) before lyophilisation.

**Characterisation of degraded PGGA and NHS-activated PGGA**

Molecular weight (MW) of degraded PGGA was determined by Gel Permeation Chromatography (GPC)  using a Viscotek Trisec Dual Detector Model 270 based on methacrylic salt 10,300 Da as a standard.  Physicochemical properties of degraded

PGGA were compared against the parent PGGA by Fourier Transmission Infra-Red (FT-IR) spectroscopy using a Perkin Elmer Spectrum 100 FTIR spectrometer; data were processed using Spectrum Express V.1.2.0 software. NHS-activated PGGA was analysed for its NHS content by $^{1}$H-NMR spectroscopy using a Bruker Advance spectrometer operating at a nominal $^{1}$H frequency of 400 MHz and equipped with a 6 mm BBO probe inducing Z-axis pulse field gradients. Spectra were processed using TOPSPIN 1.3 software.

**Characterisation of AmB/PGGA complex**

Drug loading efficiency and aggregation state of AmB were ascertained by UV-Vis spectroscopy. TEM analysis was performed to analyse size and shape of the complex. The hydrodynamic particle size and zeta potential of the AmB/PGGA complexes were determined by Dynamic Light Scattering (DLS) technique using a Zetasizer Nano ZS instrument (Malvern). Interactions between PGGA and AmB were analysed by HPLC using an Agilent Zorbax SB-C18 analytical column.

**Stability of AmB/PGGA complexes in solution**

The effect of storage conditions on the stability of AmB/PGGA complexes in solution after reconstitution in water was assessed over a 4-week period at 2-8° and room 25°C.

**_In-vitro_ antifungal activity of AmB/PGGA complexes**

Antifungal activities of the AmB/PGGA complexes were evaluated by Minimal Inhibitory Concentration (MIC) and Minimum Fungicidal Concentration (MFC) determinations, according to the guidelines by the Subcommittee on Antifungal Susceptibility Testing of the NCCLS.

**Haemolysis assay**

Preliminarily, acute drug toxicity was assessed through _in vitro_ erythrocyte lysis test, wherein hemoglobin released as a result of membrane leakage or disruption caused by exposure to the drug formulation was measured.

**Modulation of pro-inflammatory cytokines**

PBMC were incubated with test samples (AmB/PGGA complexes of 55 kDa and 110 kDa, Fungizone and AmBisome) at various concentrations for 24 h at 37°C and 5% $CO_2$. After incubation for 24 h, the supernatants were collected and immunoassayed for the determination of the cytokines TNF-α and IL-1β using immunoassay kits Human TNF-α and IL-1β ELISA Ready-SET Go (eBioscience).

**Assessment of antifungal efficacy *in vivo***

The antifungal efficacies of various AmB formulations were assessed by monitoring the survival of the infected animals and determining the clearance of *C. albicans* from various vital organs *viz.* liver, spleen and kidney. In each experiment, the infected animals were divided in 7 different groups with each group comprising of 20 animals. The animals were administered with the control (PBS), or polymer (PGGA 55 kDa and PGGA 110 kDa), or a single dose of 5 mg/kg body weight of various AmB formulations via the subcutaneous route [Fungizone, AmBisome, AmB/PGGA complex (55 kDa), AmB/PGGA complex (110 kDa)]. For survival studies, the mortality of the animals was observed twice each day during 50 days of observation. Antifungal treatment was begun 24 h after challenge of animals with *C. albicans* infection. Two animals from each group were sacrificed on day 7, 15 and 21 post-infection and pathogen burden was ascertained in vital organs.

*Statistical analysis:* data were analyzed by the Student's t-test and one way analysis of variance (Holm-Sidak method), using Sigma-Plot version 10 software. P-values <0.05 were considered to be statistically significant.

**Supplementary section:** Please refer to the Supplement for more details on Materials and Methods, physicochemical characterisations, cytotoxicity and *in vitro* antifungal evaluations, as well as additional figures.

**RESULTS**

**Degradation of PGGA**

*Molecular weight determination by Gel Permeation Chromatography (GPC):* The results of PGGA degradation are shown in Table 1. For the determination of molecular weight (MW) of the PGGA, the  specific refractive index (dn/dc) of the

polymer was obtained from a plot of refractive index (IR) detector peak area versus the PGGA concentration (0 – 10 mg/mL) at a fixed volume (1 mL); the slope of which corresponded to the dn/dc value (0.0939) (Figure S1). The polymer MW was calculated using the Rayleigh equation:

$$R(\theta)|_{\theta \to 0} \cong KCM$$

Where R, K, C and M are the intensity of the scattered light, the optical constant, the concentration and MW of the polymer, respectively.

**Table 1. Molecular weight reduction of PGGA Starting polymer MW = 1500 kDa. Data are pooled from three separate experiments (N=3).**

*Analysis of degraded PGGA by FT-IR:* Figure 1 shows the FT-IR spectra of the parent and degraded PGGA polymers, which are identical, except the parent PGGA produces higher intensity bands. The FT-IR spectra show a band at 3271.50 cm$^{-1}$ which is characteristic of the N-H stretch, whilst a band that is indicative of the COOH group appears at 1446.06 cm$^{-1}$. In addition, the absence of additional peaks suggests that the degraded PGGA was of high purity.

**Figure 1. FT-IR spectra of the parent and degraded PGGA. Parent PGGA (red bottom line) and degraded PGGA (other lines). The main peaks are N-H (3271.50 cm$^{-1}$) and COOH (1446.06 cm$^{-1}$).**

*N*-Hydroxysuccinimide (NHS) activation of PGGA

*Determination of NHS activation:* The extent of NHS activation was determined using $^1$H-NMR. Figure S2B shows an example of a $^1$H-NMR spectrum of NHS-activated PGGA. The peak at 2.8 ppm corresponds to the protons of NHS; this peak is present in the final product in contrast to that of the starting polymer (Figure S2A), and is further downfield compared to the reference NHS peak (2.6 ppm, not shown) indicating that the NHS moiety is now coupled to the polymer. In addition, the proton which corresponds to the α-carbon now appears downfield (4.15 ppm to 4.64 ppm), which provides further evidence that the NHS has coupled to PGGA. Using varying amounts of reactants, it was possible to achieve up to 91% of NHS substitution (Table 2).

**Table 2. NHS activation of PGGA. The degree of NHS activation was estimated by $^1$H-NMR. Data are means of triplicates ± SD (N=3).**

## Characterisation of AmB/PGGA complex

AmB theoretical and practical loading efficiencies of AmB/PGGA complexes are between 69.9-76.9% and 29.5-34.7%, respectively (Table 3). The complex appears spherical in structure (Figure 2A) and the particle size is distributed between 20-40 nm in diameter (TEM (JEOL), magnification x 135000 at 120 kV). Figures 2B and 2C show the size and zeta potential of a sample complex in solution. The hydrodynamic diameter of the AmB/PGGA complexes (55, 65 and 110 kDa) ranges between 96.3 – 122.5 nm with a zeta potential between -45.5 to -51.0 mV (Table 3).

**Figure 2. Size and shape characterization of AmB/PGGA complex: (A) Morphology of by TEM; (B) Size and (C) zetapotential by DLS.**

**Table 3. Drug loading efficiency; size and zeta potential of AmB/PGGA complexes by DLS. Data are means of triplicates ± SD (N=3).**

## UV Spectroscopy Analysis

The UV spectra of the AmB/PGGA complex, Fungizone and AmBisome are shown in Figure 3. In Fungizone, AmB exists predominantly as oligomeric aggregated species with a maximum absorption at 328 nm, whereas in the AmB/PGGA complex and AmBisome, AmB exists mostly as superaggregates with a maximum absorption at 322 nm.

**Figure 3.UV spectra of AmB/PGGA complex, Fungizone and AmBisome.**

## Stability of AmB/PGGA complexes in solution

The stability of AmB/PGGA complexes in solution after reconstitution in water was assessed over a 4-week period at refrigerated (2-8°) and room (25°C) temperatures (Table 4). After 1 week, ≥98% AmB was retained within the both complexes at both temperatures. After 4 weeks, ≥91% AmB was found to remain associated with the polymer. In fact, both samples remained stable for 3 weeks when stored at 2-8°C whilst

solutions stored at 25°C lost >10% of AmB content by week 4. The data suggests that the stability of the complex is greater at 2-8°C.

**Table 4. Size distribution of AmB/PGGA complexes and % AmB retained in complex at week 0,1,2,3 and 4 at 4°C and 25°C. Data are means of triplicates ± SD (N=3).**

## Analysis of interaction between AmB and PGGA by HPLC

Figure S3 shows the elution times for AmB/PGGA and AmB which are 10.2 and 10.19 min, respectively. The HPLC column used was a reverse phase hydrophobic affinity column (Agilent Zorbax SB-C18). The near identical elution times for AmB/PGGA and AmB suggest that the PGGA carrier did not affect the interaction between the AmB molecule of the AmB/PGGA complex and the HPLC column.

## Haemolysis assays

Haemolytic activity of AmB/PGGA complexes, AmBisome and Fungizone were evaluated at 1 and 24 h as shown in Figure 4A and Figure 4A respectively. Haemolysis was found to be AmB concentration-dependent, with Fungizone having the highest haemolytic activity, followed by AmB/PGGA complexes (with the lower polymer MW causing the higher haemolysis) and AmBisome, for both 1 and 24 h assays. Haemolysis was determined at time t = 1 and 24 h, expressed as % haemolysis at $\lambda$ = 580 nm.

**Figure 4. Haemolytic activity of AmB/PGGA complexes, AmBisome and Fungizone after (A) 1 h and (B) 24 h of incubation with human red blood cells. Data are means of triplicates ± SD (N = 3).**

## Evaluation of *in vitro* antifungal activity

The antifungal activity of AmB formulations was evaluated by performing MIC and MFC determinations at the AmB concentration range of 0.03-16 µg/mL (original conc. = 32 µg/mL) with an inoculum size of ~1 x $10^4$ CFU. Table 5 shows the MICs and MFCs at 24 and 48 h; and 48 h, respectively. Overall, MIC and MFC values of all AmB/PGGA complexes, Fungizone and AmBisome were consistently equal or one-

fold dilution higher or lower than those recorded for AmB. PGGA alone had no antifungal activity.

**Table 5. MICs and MFCs of AmB/PGGA complexes, Fungizone, AmBisome and AmB against** *Candida spp*.**, expressed as (μg/mL). Data are modal values of 3 independent measurements. Range varied no more than two-fold from stated values in each case.**

## Modulation of pro-inflammatory cytokine production

Regulation of the cytokines TNF-α and IL-1β was evaluated for AmB/PGGA complexes against the comparators, AmBisome and Fungizone (Figures 5A and 5B). There were no significant differences between the formulations except for Fungizone, which caused the highest upregulation for both cytokines at the highest AmB concentration tested (2 μg/mL).

**Figure 5. Cytokine release as a function of AmB concentration, produced by PBMCs in the presence of various AmB formulations: (A) TNF-α; (B) IL-1β. Data are means of triplicates (N=3).**

## Evaluation of *in vivo* antifungal efficacy

The efficacy of AmB/PGGA complexes was evaluated in mice infected with *C. albicans* and were compared against Fungizone and AmBisome, with PBS as a control. Figure 6 shows that both AmB/PGGA C55 kDa and C110 kDa complexes were significantly more efficacious, as compared with Fungizone and AmBisome [C55 kDa and C110 kDa complexes versus Fungizone (p<0.001) and AmBisome (p<0.001)]; and C110 kDa was significantly more efficacious than C55 kDa (p<0.001). Assessments of fungal load in vital organs (spleen, liver and kidneys) after treatment with AmB formulations also confirmed that overall, AmB/PGGA complexes were more efficacious than Fungizone and AmBisome, with the higher MW complex having the greater efficacy (Figures 7A, 7B, and 7C).

**Figure 6. Survival percentage of animals infected with *C. albicans* cells ($10^7$ CFU) over 50 days post-treatment (PGGA 55 kDa = PGGA polymer of MW 55k Da alone, PGGA 110 kDa = PGGA polymer of MW 110 kDa alone, C 55 kDa = AmB/PGGA complex with MW 55 kDa, C 110 kDa = AmB/PGGA complex with MW 110 kDa).**

12

**Figure 7. Assessment of fungal load in vital organs of infected animals; (A) spleen (B) liver and (C) kidney (PGGA 55 kDa = PGGA polymer of MW 55k Da alone, PGGA 110 kDa = PGGA polymer of MW 110 kDa alone, C 55 kDa = AmB/PGGA complex with MW 55 kDa, C 110 kDa = AmB/PGGA complex with MW 110 kDa).**

## DISCUSSION

Our goal was to develop an alternative AmB formulation that offers the best attributes of the approved AmB formulations, namely the high efficacy and low cost of the AmB-deoxycholate, along with improved safety profiles of the lipid based AmB formulations. Using the naturally-occurring and biodegradable polymer PGGA, we were able to synthesize non-covalently associated AmB/PGGA complexes of varying polymer molecular weights (55, 65 and 110 kDa). The preparation of the AmB/PGGA complexes involved three main processes: firstly, the MW reduction of the high MW PGGA by alkaline hydrolysis; secondly, the hydrophobisation of the reduced PGGA via NHS activation to increase its organic solubility; and thirdly the preparation of complexes through solubilisation of drug and polymer in an organic medium (DMSO), followed by alkaline hydrolysis. Using varying amounts of reactants, it was possible to achieve lower MW polymer (Table 1), with high purity as shown by F-TIR (Figure 1); and up to 91% of NHS substitution (Table 2). As the drug and polymer underwent alkaline hydrolysis and transitioned from an organic medium to a predominantly aqueous medium, it was observed that the water-soluble AmB/PGGA complexes formed spontaneously, possibly via a mechanism of self-assembly. Although we did not verify this, PGGA or its derivatives have been known to form self-assembled, nano-sized particles [32]. Several researchers have demonstrated the self-assembly formation of nano-carriers based on PGGA [33], [34]; with one recent study confirming the self-assemblage of PGGA nanoparticle by measuring CMC (critical micelle concentration) using pyrene as a hydrophobic probe [35]. In general, polymeric nanoparticles are often formed through self-assembly [36], a process driven by the hydrophobic, hydrophilic and amphiphilic characteristics of the different (co)polymers. In contrast to conjugation methods, which often requires complex coupling chemistry, our method is comparatively simpler and highly efficient, achieving a consistent practical loading of 26.1 to 34.7% (w/w) (Table 3), which compares well against 3.8% (w/w) and 45.5%

(w/w) for AmBisome and Fungizone, respectively. The data suggests that AmB/PGGA complexes can be formulated using only PGGA and no other excipients; this is an advantage over products that require many stabilising agents, since these excipients may cause toxicity and/ or incompatibility issues [37].

Lyophilised AmB/PGGA complexes were found to be readily soluble in water, resulting in a clear solution.  In contrast, the reconstitution of both AmBisome and Fungizone involves a more complicated procedure that requires vigorous shaking, inspection or dilution [6], [7].  TEM imaging of the AmB/PGGA complexes revealed a uniform population of spherical nanoparticles with a mean diameter of 20-40 nm (Figure 2). The morphology of the complexes is similar to that reported by Yoo et al. which, according to the author, is indicative of a polymeric micellar system [38]. It was hypothesised that the interaction between the carrier (PGGA) and the drug (AmB) was likely to be of a non-covalent nature. To test this hypothesis, the AmB/PGGA complex and the free AmB were analysed by HPLC using a hydrophobic column. As shown in Figure S3, the elution times were similar between the AmB/PGGA complex and the free AmB, indicating that the interactions of AmB in the complex with a hydrophobic affinity column were therefore not affected by the forces that hold the polymeric carrier (PGGA) and AmB together.  This suggests that the interactions between the PGGA and AmB were non-covalent rather than covalent because the latter would have affected the elution time of the AmB/PGGA complex.

Non-covalent complexes are known to suffer from the possible risk of drug loss from the drug carrier due to the weaker forces that hold the drug and the drug carrier as compared with a covalent drug-conjugate.  We, therefore, investigated the stability of the AmB/PGGA complexes (55 and 110 kDa) in solution and found that both AmB/PGGA complexes retained more than 90% of AmB at 4°C, and more than 86% of AmB at 25°C, after 4 weeks (Table 4). The apparent high stability of the AmB/PGGA in solution could be due to the negative charge and the nanoscopic range of the complexes ($\sim$-50 mV, and 90 – 120 nm as measured by DLS, respectively) (Table 3). Previous studies have reported that small and negatively charged particles have high stability, reduced interactions with blood components, as well as greater passive targeting and longer blood residence time [39], [40]. Extremely positive or negative zeta potential values cause larger repulsive forces; this repulsion between similarly charged particles prevents aggregation of the particles and thus maintains a stable

14

system [41]. Polymeric systems, such as the AmB/PGGA complexes, are characterised by greater thermodynamic stability, as evidenced by their lower CMCs than smaller surfactants, thereby offering high resistance to dissociation [42]. On the contrary, as per label, Fungizone should be stored for no more than 8 hours at room temperature (25°C) or 24 hours in a refrigerator (2-8°C), and the in-use storage time of AmBisome would normally not be longer than 24 h at 2-8°C [6], [7]. A study assessing the stability of Fungizone solutions has reported up to 20% loss of AmB after 1 h incubation at 37°C due to auto-oxidation processes and colloidal instability [43], [44].

AmB is known to interact freely with the cholesterol in red blood cells leading to severe haemolysis [45], [46]. Haemolysis assays at 1 and 24 hours demonstrated that all three AmB/PGGA complexes caused significantly less haemolysis than Fungizone but greater than AmBisome, and the AmB/PGGA complex with the higher MW polymer to be less haemolytic (110 kDa< 65 kDa<55 kDa) (Figure 4). Fungizone is highly haemolytic because it is formulated with the excipient, sodium deoxycholate, an anionic surfactant known to cause haemolysis [58]. Previously, low haemolytic activity has been attributed to the superaggregated form of AmB, found in AmBisome and in the heated solution of Fungizone; as indicated by a UV spectral shift of the maximum absorption from 328 nm to 322 nm [43]. Figure 3 confirms that AmB/PGGA complex too contains the superaggregated form of AmB, which is in accordance with a study conducted on a AmB formulation developed with a variant of PGA (poly L-glutamic acid) [46], and thus provides an explanation for the observed lowered haemolytic activity of the AmB/PGGA complexes. It has been suggested that the regulated release of AmB from the polymer maintains the released drug in a monomeric form (since the concentration of the released drug remains below its CMC for aggregation), preventing it from forming oligomeric aggregates. Both monomer and super-aggregate forms of AmB are less toxic, while the oligomeric species are mainly responsible for the drug induced toxicity [47]. Moreover, only small amount of drug is available to bind to the red blood cell membrane due to the slow release, thereby reducing toxicity; although this is yet to be tested experimentally.

The formulation process of the AmB/PGGA complexes did not affect the AmB structure, as evidenced by the antifungal efficacy of the AmB/PGGA complexes in *vitro* against *Candida albicans ATCC 14053* and *Candida tropicalis ATCC 750* and demonstrated similar efficacy as compared with Fungizone and AmBisome. The MFC

15

values of the AmB/PGGA complexes were also comparable to those of Fungizone and AmBisome (0.5-1 μg/mL) (Table 5).

The administration of conventional AmB is often associated with infusion-related toxicity side effects such as fever and chills, as a result of the upregulation of proinflammatory cytokines, TNF-α and IL-1β [48], [49]. In human peripheral blood mononuclear cells (PBMCs), it was found that Fungizone upregulated the production of both TNF-α and IL-1β, whereas the two AmB/PGGA complexes (55 and 110 kDa) and AmBisome did not (Figure 5). These findings also indirectly confirm clinical experience which reports greater incidence rates of infusion-related toxicity for Fungizone than AmBisome [48]. Based on these findings, it is reasonable to expect that AmB/PGGA complexes may have similar incidence rates of the aforementioned toxicity as with AmBisome.

The antifungal efficacy of two AmB/PGGA complexes was evaluated in experimental murine candidiasis. AmB/PGGA complexes were found to be more effective in clearing fungal burden in liver, spleen and kidney of infected animals than both Fungizone and AmBisome (Figure 7). The greater antifungal efficacies of the AmB/PGGA complexes were further established in our survival studies in which the AmB/PGGA complexes out-performed both Fungizone and AmBisome by a significant margin. Fifty days post treatment, the survival rates for the animals receiving the AmB/PGGA complex (110 kDa), the AmB/PGGA complex (55 kDa), AmBisome and Fungizone were 80%, 50%, 30% and 0%, respectively (Figure 6). Our data suggest that the AmB/PGGA complexes have a higher antifungal efficacy than both comparators.

The mechanism by which the AmB/PGGA complexes exert their greater antifungal efficacy is not known, although it has been suggested that the incorporation of PGGA into chitosan/siRNA and chitosan/DNA complexes enhances their cellular uptake and facilitates the unpacking of the complexes to release the payload upon cell entry [50], [51]. It has also been reported that necrotizing vasculitis occurs during *Candida* infections [52] and the leaky blood vessels at these sites of inflammation may result in enhanced permeation of nanocarriers [53]. Overall, colloidal polymeric carriers including PGGA [10], [11], [12], are naturally passively targeted to, or can be tailored to actively target, organs of reticuloendothelial system (RES); leading to greater distribution of AmB to liver and spleen, thereby effectively reducing the pathogen burden [16]. Biodistribution studies have shown that (passively targeted)

Amphocil® and Abelcet® are rapidly accumulated in the mononuclear phagocyte system [54]. Incidentally, macrophages are heavily involved in inflammation and pathogenesis of many diseases such as candidiasis [55]; thus may act as 'Trojan horses' [56] and carry encapsulated nanoparticles to the site of infection. Subsequently, nanoparticle-bearing macrophages may act as 'secondary depot' or 'cellular drug reservoirs' of active drug entities [57], gradually releasing it into the surrounding milieu [58]. Thus, macrophages may provide an indirect boost to microbial clearance as the drug can be delivered to the site of active pathogen growth [59]. Although initially demonstrated in cancer, this paradigm may be extended to other nano-encapsulated therapeutics and non-cancer disease indications [60] in which macrophages accumulate near the target tissue. It seems, therefore, plausible that PGGA, in a fashion similar to other polymeric nanocarriers, facilitate the passive targeting of AmB via macrophages to the site of infection; this may explain the enhanced antifungal efficacy (Figure 6 and 7) as well as the reduced toxicity of the AmB/PGGA complexes (Figure 4 and 5).

In conclusion, we have developed AmB/PGGA complexes that possess the potential to replace the current commercial AmB formulations. These AmB/PGGA complexes have demonstrated a number of desirable attributes including water solubility, stability, decreased cytotoxicity and improved antifungal efficiency. The relative simple formulation method and the abundance of the naturally-occurring polymer mean that if successfully realised as a medicinal product, an AmB/PGGA complex formulation could potentially be manufactured and offered at a low cost. However, although PGGA has been consumed by humans over many centuries, it is still not known whether it would elicit immunogenicity when administered parenterally. Future studies therefore should assess the immunogenicity potential of the AmB/PGGA complexes and confirm the enhanced efficacy that was observed in our animal models. In our investigations, the AmB/PGGA complex with the higher molecular weight polymer performed better than that with lower molecular weight in terms of cytotoxicity and antifungal efficacy. It is thus recommended that the higher molecular weight AmB/PGGA complexes be further investigated.

**REFERENCES**

1.      Gallis HA, Drew RH, Pickard WW. Amphotericin B: 30 years of clinical experience. Reviews Infect Dis 1990;12(2):308-329.

2.      Deray G. Amphotericin B nephrotoxicity. J Antimicrob Chemother 2002;49(Suppl 1):37-41.

3.      Inselmann G, Voss V, Kunigk F, Heidemann H. Influence of amphotericin B treatment duration of hepatic microsomal enzyme function in rats. Pharmacol 1997;55(2):87-94.

4.      Pound MW, Townsend ML, Dimondi V, Wilson D, Drew RH. Overview of treatment options for invasive fungal infections. Med Mycol 2011;49(6):561-80.

5.      Kleinberg M. What is the current and future status of conventional amphotericin B. Int J Antimicrob Agents 2006;27(1):12-6.

6.      AmBisome® Summary of Product Characteristics https://www.medicines.org.uk/emc/medicine/1236. Accessed 08-Feb-2016

7.      Fungizone® Summary of Product Characteristics https://www.medicines.org.uk/emc/medicine/559/SPC/Fungizone+50mg+Powder+for +Sterile+Concentrate/. Accessed 08-Feb-2016

8.      Girois SB, Chapuis F, Decullier E, Revol BG. Adverse effects of antifungal therapies in invasive fungal infections: review and meta-analysis. Eur J Clin Microbiol Infect Dis 2006;25(2):138-149.

9.      Zhao F, Zhao Y, Liu Y, Chang X, Chen C, Zhao Y. Cellular uptake, intracellular trafficking, and cytotoxicity of nanomaterials. Small 2011;7:1322–1337.

10.      Gupta S, Vyas SP. Development and characterization of amphotericin B bearing emulsomes for passive and active macrophage targeting. J Drug Target 2007; 15(3): 206–217

11.      Melancon MP, Li C. Multifunctional synthetic poly(L-glutamic acid)-based cancer therapeutic and imaging agents. Mol Imag 2011;10(1):28-42.

12.      Yoo J-W, Irvine D J., Discher D E. & Mitragotri S. Bio-inspired, bioengineered and biomimetic drug delivery carriers. Nature Reviews Drug Discov 2011; 10, 521-535.

13.      Torchilin VP. Multifunctional, stimuli-sensitive nanoparticulate systems for drug delivery. Nature reviews Drug Discov 2014;13(11):813-827.

14.      Sedlák M, Pravda M, Staud F, Kubicová L, Týcová K, Ventura K. Synthesis of pH-sensitive amphotericin B-poly(ethylene glycol) conjugates and study of their controlled release in vitro. Bioorg Med Chem 2007;15(12):4069-76.

15. Vyas SP, Quraishi S, Gupta S, et al. Aerosolized liposome-based delivery of amphotericin B to alveolar macrophages. Int J Pharm 2005;296:12–25.

16. Veerareddy PR, Vobalaboina V, Ali N. Antileishmanial activity, pharmacokinetics and tissue distribution studies of mannose grafted amphotericin B lipid nanospheres. J Drug Target 2009;17:140-7

17. Vandermeulen G, Rouxhet L, Arien A, Brewster ME, Preat V. Encapsulation of amphotericin B in poly(ethylene glycol)-block-poly(ε-caprolactone-co-trimethylene carbonate) polymeric micelles. Int J Pharm 2006;309:234–240.

18. Zia Q, Farazuddin M, Ansari MA, Alam M, Ali A, Ahmad I, Owais M. Novel drug delivery systems for antifungal compounds, pgs 485-528, In: Combating Fungal Infections: Problems and Remedy, (Eds; Iqbal Ahmad, M Owais, M Shahid, F Aqil). Springer-Verlag Berlin Heidelberg 2010.

19. Jee J, McCoy A, Mecozzi S. Encapsulation and release of Amphotericin B from an ABC triblock fluorous copolymer. Pharm Res 2012;29: 69-82.

20. Chen H, Kim S, He W, Wang H, Low PS, Park K, Cheng JX. Fast release of lipophilic agents from circulating PEG-PDLLA micelles revealed by in vivo forster resonance energy transfer imaging. Langmuir 2008;24(10):5213–5217.

21. Savic R, Azzam T, Eisenberg A, Maysinger D. Assessment of the integrity of poly(caprolactone)-b-poly(ethylene oxide) micelles under biological conditions: A fluorogenic-based approach. Langmuir 2006;22(8):3570–3578.

22. Xu XY, Zhang XF, Wang XH, Li YX, Jing XB. Comparative study of paclitaxel physically encapsulated in and chemically conjugated with PEG-PLA. Polymers Adv Technol 2009;20(11):843–848.

23. Espuelas MS, Legrand P, Campanero MA, Appel M, Chéron M, Gamazo C, Barratt G, Irache JM. Polymeric carriers for amphotericin B: in vitro activity, toxicity and therapeutic efficacy against systemic candidiasis in neutropenic mice. J Antimicrob Chemother 2003;52:419–427.

24. Charvalos E, Tzatzarakis MN, Van Bambeke F, et al. Water soluble amphotericin B-polyvinylpyrrolidone complexes with maintained antifungal activity against *Candida* spp. and *Aspergillus* spp. and reduced haemolytic and cytotoxic effects. J AntimicrobChemother 2006; 57:236–244.

25. Jansook P, Loftsson T. CDs as solubilizers: effects of excipients and competing drugs. Int J Pharm 2009;379:32–40.

26.     Ohtani Y, Irie T, Uekama K, Fukunaga K, Pitha J. Differential effects of alpha-, beta- and gamma-cyclodextrins on human erythrocytes. Eur J Biochem 1989;186:17–22.

27.     Kopecek J, Kopecková P, Minko T, LuZR, Peterson CM. Water soluble polymers in tumor targeted delivery. J Control Release 2001;74(1-3):147-58.

28.     Kedia G, Hill D, Hill R, Radecka I. Poly-γ-glutamic acid: production, properties and applications. J Nanosci Nanotechnol 2010;10(9):5926-34.

29.     Prodhomme EJ, Tutt AL, Glennie MJ, Bugg TD. Multivalent conjugates of poly-gamma-D-glutamic acid from *Bacillus licheniformis* with antibody F(ab') and glycopeptide ligands. Bioconjug Chem 2003;14(6):1148-55.

30.     Akagi T, Kaneko T, Kida T, Akashi M. Multifunctional conjugation of proteins on/into bio-nanoparticles prepared by amphiphilic poly(gamma-glutamic acid). J Biomater Sci Polym Ed 2006;17:875–892

31.     Luo Z , Y Guo, J Liu, H Qiu, M Zhao, W Zou. and S Li. Microbial synthesis of poly-γ-glutamic acid: current progress, challenges, and future perspectives. Biotech Biofuels 2016; 9:134.

32.     Akagi T, Matsusaki M, Akashi M. Pharmaceutical and medical applications of poly-gamma-glutamic acid. In: Amino-acid homopolymers occurring in nature. Y. Hamano (ed.), Microbiology Monographs 15, pg 119-153. DOI: 10.1007/978-3-642-12453-2_7. Springer-Verlag 2010.

33.     Zhu Y, Akagi T. and Akashi M. Self-assembling stereocomplex nanoparticles by enantiomeric poly(γ-glutamic acid)-poly(lactide) graft copolymers as a protein delivery carrier. Macromol Biosci 2014;14:576–587. doi: 10.1002/mabi.201300434.

34.     Meng L, Ji B, Huang W, Wang D, Tong G, Su Y, Zhu X, Yan D. Preparation of pixantrone/poly(γ-glutamic acid) nanoparticles through complex self-assembly for oral chemotherapy. Macromol Biosci 2012;12(11):1524-33.

35.     Liu M, Huang G, Cong Y, Tong G, Lin Z, Yin Y, Zhang C. The preparation and characterization of micelles from poly(γ -glutamic acid)-graft-poly(L-lactide) and the cellular uptake thereof. J Mater Sci: Mater Med 2015;26:187.

36.     Lameijer MA, Tang J, Nahrendorf M, Beelen RHJ, Mulder WJM. Monocytes and macrophages as nanomedicinal targets for improved diagnosis and treatment of disease. Expert Review Mol Diagnos 2013;13(6):567-580.

37.     Nema S, Brendel RJ. Excipients and their role in approved injectable products: current usage and future directions. PDA J Pharm Sci Technol 2011; 65(3):287-332.

38.     Yoo HS, Park TG. Biodegradable polymeric micelles composed of doxorubicin conjugated PLGA-PEG block copolymer. J Control Release 2001;70(1-2):63-70.

39.     Alexis F, Pridgen E, Molnar LK, Farokhzad OC. Factors affecting the clearance and biodistribution of polymeric nanoparticles. Mol Pharm 2008;5(4):505-15.

40.     Kataoka K, Matsumoto T, Yokoyama M, Okano T, Sakurai Y, Fukushima S, Okamoto K, Kwon GS. Doxorubicin-loaded poly(ethylene glycol)-poly(beta-benzyl-L-aspartate) copolymer micelles: their pharmaceutical characteristics and biological significance. J Control Release 2000;64:143–153.

41.     Patila et al 2007. Patila S, Sandberg A, Heckert E, Self W, Sea S. Protein adsorption and cellular uptake of cerium oxide nanoparticles as a function of zeta potential. Biomaterials 2007;28:4600–4607.

42.     Biesendorfer H, Felix W, Wildenauer DB. Studies on the haemolytic action of amphiphilic substances in vitro: Inhibition by O-(beta-hydroxyethyl)-rutosides. Biochem Pharmacol 1981;30(16):2287-92.

43.     Gaboriau F, Chéron M, Leroy L, Bolard J. Physicochemical properties of the heat-induced 'superaggregates' of amphotericin B. Biophys Chem 1997;66(1)1-12.

44.     Larabi M, Pages N, Pons F, Appel M, Gulik A, Schlatter J, et al. Study of the toxicity of a new lipid complex formulation of amphotericin B. J Antimicrob Chemother 2004;53(1):81-88.

45.     Hsuchen CC, Feingold DS. Selective membrane toxicity of the polyene antibiotics: studies on natural membranes. Antimicrob Agents Chemother 1973;4(3):316-9.

46.     Zia Q, Khan AA, Zubair S, Owais M. Self-assembled amphotericin B loaded poly-glutamic acid nanoparticles: Preparation, characterization and in vitro potential against *Candida albicans.* Int J Nanomed 2015;10:1769–1790.

47.     Zia Q, Azhar A, Kamal MA, Aliev G, Owais M, Ashraf GM. Super aggregated form of amphotericin B: a novel way to increase its therapeutic index. Current Pharmaceu Design 2016; 22(7): 792-803

48.     Walsh TJ, Finberg RW, Arndt C, Hiemenz J, Schwartz C, Bodensteiner D, et al. Liposomal amphotericin B for empirical therapy in patients with persistent fever and

neutropenia. Nat Inst Allergy Infect Dis, Mycoses Study Group. New Eng J Med 1999;340(10):764-71.

49.     Tokuda Y, Tsuji M, Yamazaki M, Kimura S, Abe S, Yamaguchi H. Augmentation of murine tumor necrosis factor production by amphotericin B in vitro and in vivo. Antimicrob Agents Chemother 1993;37(10):2228-30.

50.     Liao ZX, Ho YC, Chen HL, Peng SF, Hsiao CW, Sung HW. Enhancement of efficiencies of the cellular uptake and gene silencing of chitosan/siRNA complexes via the inclusion of a negatively charged poly(γ-glutamic acid). Biomaterials 2010;31(33):8780-8788.

51.     Peng S F, Tseng MT, Ho YC, Wei MC, Liao ZX, Sung HW. Mechanisms of cellular uptake and intracellular trafficking with chitosan/DNA/poly(γ-glutamic acid) complexes as a gene delivery vector. Biomaterials 2011;32(1):239-48.

52.     Guarner J, Brandt ME. Histopathologic diagnosis of fungal infections in the 21st century. Clin Microbiol Rev 2011;24(2): 247–280.

53.     Hossain M A, Maesaki S, Kakeya H, Noda T, Yanagihara K, Sasaki E, Hirakata Y, Tomono K, Tashiro T, and Kohno S. Efficacy of NS-718, a novel lipid nanosphere-encapsulated amphotericin B, against *Cryptococcus neoformans*. Antimicrob. Agents Chemother 1998; 42(7):1722-1725.

54.     Barratt G and Bretagne S. Optimizing efficacy of amphotericin B through nanomodification. Int J Nanomed 2007:2(3) 301–313.

55.     Weiss G, Schaible UE. Macrophage defense mechanisms against intracellular bacteria. Immunol Rev 2015;264: 182–203.

56.     Pang L, Qin J, Han L, ZhaoW, LiangJ, Xie Z, Yang P, Wang J. Exploiting macrophages as targeted carrier to guide nanoparticles into glioma. Oncotarget 2016;7(24):37081-37091.

57.     Miller MA, Zheng Y-R, Gadde S, Pfirschke C, Zope H, Engblom C et al. Tumour associated macrophages act as a slow-release reservoir of nano-therapeutic Pt(IV) pro-drug. Nature Comm 2015;6: 8692.

58.     Fu J, Wang D, Mei D, Zhang H, Wang Z, He B, Dai W, Wang X, Zhang Q. Macrophage mediated biomimetic delivery system for the treatment of lung metastasis of breast cancer. J Control Release 2015; 204:11–19.

59.     McMillan J, Batrakova E, Gendelman HE. Cell delivery of therapeutic nanoparticles. Prog Mol Biol Transl Sci 2011;104:563-601.

60.    Klyachko NL, Haney MJ, Zhao Y, Manickam DS, Mahajan V, Suresh P, Hingtgen SD, Mosley RL, Gendelman HE, Kabanov AV, Batrakova EV. Macrophages offer a paradigm switch for CNS delivery of therapeutic proteins. Nanomed (Lond) 2014; 9:1403–1422.